*Environ. Sci. Technol.* **2010,** *44,* 5423–5429

# Temperature and Hydrologic Controls on Dissolved Organic Matter Mobilization and Transport within a Forest Topsoil

NA XU* AND JAMES E. SAIERS

*School of Forestry and Environmental Studies, Yale University, New Haven, Connecticut, 06511*

*Received January 21, 2010. Revised manuscript received May 26, 2010. Accepted June 2, 2010.*

Variations in concentrations of dissolved organic matter (DOM) in streams and rivers reflect, in part, coupled biogeochemical and hydrological processes that govern DOM mobilization and transport through soils. We explore the effects of temperature and rainfall characteristics on the quantity and composition of DOM mobilized from laboratory columns packed with an unsaturated forest soil. Our observations demonstrate that changes in temperature and a five-month drought period affect the mass and structure of DOM mobilized during soil−water infiltration, while changes in rainfall intensity and hourly to daily changes in the frequency of rainfall affect only the mass of DOM mobilized. The spectroscopic analyses indicate that DOM mobilized at low temperature is less humified and tends to be less condensed and lower in molecular weight. The C:N ratios of effluent DOM decline with cumulative rainfall volume during successive rainfall events and decrease by an average of 36% owing to the extended drought period. A two-region model that accounts for rate-limited DOM desorption from soil−water interfaces present within inter-aggregate and intra-aggregate pore spaces closely describes the time-series data on total concentrations of DOM eluted from the soil columns during the rainfall events.

## 1. Introduction

Dissolved organic matter (DOM) plays an important role in various processes in terrestrial and aquatic ecosystems. In particular, DOM influences nutrient cycling and contaminant mobility, provides an energy source for heterotrophic production, and affects soil and water pH (*1*). DOM exported from watersheds is produced, in part, as infiltrating rainwater or snowmelt leaches organic-rich soil horizons and travels as subsurface storm flow or groundwater flow before re-emerging within or near the stream channel (*2*).

In forested catchments, a large proportion (1/3 to more than 1/2) of the annual DOM export occurs during rainfall events and both streamwater DOM concentrations and fluxes vary between seasons (*3, 4*). Several studies report higher concentrations of DOM in streamwater and soil water in the summer and fall compared to winter and spring (*5, 6*). Other studies demonstrate annual peak DOM concentrations and export during the spring snowmelt (*4*). Many factors contribute to this range in DOM-export behavior, including, but not limited to, the interactions among temperature-dependent biochemical processes that regulate the size of the DOM pool and rainfall (and snowmelt)-dependent hydrologic processes that transmit water and DOM to the stream.

DOM mobilization from soils is rate-limited and occurs by desorption, dissolution, and diffusive mass transfer from immobile to mobile water regions (*7*−*9*). Meteorological variables, such as rainfall intensity and frequency, influence soil moisture, porewater flow rates, and solute residence times and thus affect the concentrations of DOM mobilized during rainfall events. Temperature influences the production and decay of potential mobile organic matter between rainfall events by controlling microbial activity (*10*−*12*). Temperature also regulates DOM dissolution and desorption, although the sensitivity of these physicochemical processes to changes in temperature is poorly known.

The structure of DOM, in addition to its concentration, influences water quality and biogeochemistry. DOM fractions with lower molecular weight, lower aromaticity, and less condensed structure are more readily metabolized by microorganisms and have lower affinity for complexing dissolved contaminants (*13, 14*). Dissolved organic nitrogen (DON), a component of DOM, constitutes a significant portion of the total nitrogen flux for some ecosystems (*1*). A few studies have demonstrated dissimilarities in the soil−water transport behavior of DON and dissolved organic carbon (DOC) (*15*), which suggests that leaching patterns differ among components of the DOM pool. Few studies, however, have focused on elucidating how the structure of soil−water DOM varies within and between infiltration events and in response to physicochemical properties that may influence DOM mobilization.

The objectives of this study were therefore to (i) investigate the influence of temperature and rainfall characteristics on the concentrations and structure of DOM mobilized from a forest soil; (ii) evaluate the possible difference between DOC and DON dynamics; and (iii) elucidate the physicochemical mechanisms that govern DOM mobilization and transport during rainfall events. We measured the concentrations and structure of DOM mobilized from partially saturated topsoil during simulated rainfall events. The column experiments were differentiated on the basis of rainfall intensity, rainfall frequency, temperature, soil biotic activity (i.e., sterile vs unsterilized soil), and soil storage time before rainfall initiation. In addition to analyzing the column effluent for concentrations of DOC and DON, we analyzed the ultraviolet (UV) absorbance and fluorescence spectra of the water samples to evaluate how the structure of DOM changed during a precipitation event and between successive precipitation events. Finally, we applied a transport model to the DOM breakthrough data to quantify how DOM mobilization rates responded to changes in experimental conditions.

## 2. Materials and Methods

**2.1. Soil Material and Rainfall Solution Chemistry.** Soil was collected from the A horizon of an Inceptisol under a mixed coniferous stand in Harvard Forest in Petersham, MA. The field-moist soil was screened through a coarse mesh (5.6 mm) to remove stones and woody debris, while preserving some of the micropore structure within the soil aggregates. The sieved soil was homogenized by gentle mixing with a plastic spade and stored in an airtight container at 6 °C in the dark until use. The soil had a pH of 3.8 (1:2 w/w soil/water), moisture content of 51%, organic carbon content of 153 g $kg^{-1}$ (Thermo Finnigan Delta$^{Plus}$ Advantage), a C:N ratio of 26:1, and a sandy loam texture with 61% sand, 7% silt, and 32% clay.

* Corresponding author e-mail: na.xu@yale.edu.

10.1021/es1002296 
Published on Web 06/16/2010

**TABLE 1. Summary of Experimental Conditions and Model Results**

| | rainfall characteristics | | | | soil properties | | model results[c] | | |
|---|---|---|---|---|---|---|---|---|---|
| treatment | intensity (cm/h) | duration (hr) | interruption interval (hr) | $T^a$ (°C) | sterilization | storage[b] (wk) | $k_d$ ($h^{-1}$) | $\omega$ ($h^{-1}$) | $R^2$ |
| T-1 | 2.9 | 7 | 39 | 24 °C | no | 2 | 0.229 | 0.0044 | 0.95 |
| T-2 | 1.0 | 18.5 | 39 | 24 °C | no | 3.5 | 0.122 | 0.0037 | 0.945 |
| T-3 | 2.9 | 7 | 147 | 24 °C | no | 6 | 0.331 | 0.0012 | 0.943 |
| T-1′ | 2.9 | 7 | 39 | 24 °C | no | 23 | 0.297 | 0.0044 | 0.978 |
| T-5 | 2.9 | 7 | 39 | 3 °C | no | 24 | 0.103 | 0.0004 | 0.933 |
| T-7 | 2.9 | 7 | 39 | 24 °C | yes | 25 | 0.442 | 0.0016 | 0.991 |
| T-6 | 2.9 | 7 | 39 | 3 °C | yes | 25 | 0.105 | 0.0004 | 0.945 |

[a] Abbreviation for temperature. [b] Soils were stored under 6 °C in the dark, and the storage time was counted between the field sampling day and the first rainfall treatment. [c] Other parameters used in the model are presented in the Supporting Information.

A portion of the sieved soil was sterilized by gamma irradiation at a dosage rate of 500 Gy $h^{-1}$ for 50 h (MIT Nuclear Reactor Lab), which, according to Berns et al. (*16*), is sufficient to eliminate living soil microorganisms. Gamma irradiation has been recommended over other techniques for soil sterilization because it leads to less alteration of soil properties (*17*). No significant temperature fluctuation or moisture change was observed during the irradiation.

The rainfall solution used in the soil-column experiments consisted of either 0.2 mM KBr or 0.2 mM KCl, adjusted to pH 4.5 by the addition of HCl. The ionic strength and pH of the rainfall solution were similar to those of naturally occurring rainwater in the Harvard Forest. Prior to use in the column experiments, the rainfall solutions were autoclaved for 50 min at 120 °C.

**2.2. Column Design.** Field-moist soil (184 g) was packed into acid-washed, autoclaved, glass chromatography columns (Kontes) measuring 4.8 cm diameter and 15 cm long. Fresh columns were packed for each experiment by adding soil in 46-g increments and tapping the sides of the column a uniform number of times between each incremental addition to settle the soil. A 0.5-cm-thick layer of acid-washed quartz sand (0.71−0.85 mm) was placed on the soil surface to ensure the rainfall was evenly dispersed over the top of the soil column. A fritted glass plate with ~15 $\mu$m pores (Chemglass Inc.) was emplaced at the base of the column to support the soil and permit the passage of soil leachate. To prevent soil particles from clogging the plate, a 1-cm-thick layer of sand was placed between the soil and glass plate (*18*). The bulk density and pore volume of the soil columns equaled 0.36 g $cm^{-3}$ and 175 $cm^3$, respectively.

To maintain unsaturated flow, 10 cm of tension was applied at the column base with a hanging water column. Tensiometers (consisting of ceramic cups, Soil Moisture Corp.) connected to differential microtransducers (Honeywell/Microswitch) for monitoring capillary pressure head were located at 3.5, 7, 10.5, and 13.5 cm from the top of the column. Data from the tensiometers were collected using a datalogger (Delta-T Devices, Ltd.). A peristaltic pump (Cole-Parmer Instrument Co.) was used in conjunction with Tygon tubing (sterilized with peracetic acid) to apply the rainfall solutions to the soil at known rates. Column effluent samples were collected with a fraction collector (Spectra/Chrom) and analyzed for DOM concentration and structure as described in Section 2.4. During periods of rainfall interruption, a rubber stopper was placed on top of the glass column to reduce evaporation.

**2.3. Experimental Treatments.** Seven experiments were conducted in duplicate and differentiated on the basis of rainfall intensity, rainfall frequency (i.e., interruption interval between successive events), temperature, soil biotic activity (i.e., sterile vs unsterile soil), and soil storage time before rainfall initiation (Table 1). The rainfall intensities and interruption intervals varied from 1 to 2.9 cm $h^{-1}$ and 39 to 147 h, respectively, and fall within the range of naturally occurring rainfall events at the Harvard Forest. Five experiments were conducted at 24 °C and two experiments were conducted at 3 °C (Table 1). For the low-temperature treatments, the column and artificial rainfall reservoirs were placed in a frost-free freezer (GE), where temperature was controlled by a freezer thermostat (KegMan LLC). Temperature fluctuations did not exceed ±1 °C in any experiment. Preliminary tests confirmed negligible change to the soil organic matter pool within 2 weeks of storage in the dark at 6 °C, but that storage over greater time periods affected the soil organic matter pool. For this reason, two base-case (reference) experiments (T-1 and T-1′) were conducted so that comparison between treatments could be made on experiments conducted within a 2-week time period (Table 1).

All soil columns were let stand for 38 h after packing to allow soil-moisture conditions to stabilize and then subjected to three separate rainfall events, each consisting of 364 mL of the electrolyte solution. Most rainfall events lasted 7 h except for those of treatment T-2, which lasted 18.5 h (Table 1). The 0.2 mM KBr solution (see above) was applied during the first half of each rainfall event, and the equimolar KCl solution was applied for the second half of the event.

**2.4. Characterization of Column-Effluent Samples.** Effluent samples were collected from the base of the column throughout each experiment and filtered through 0.45-$\mu$m polyethersulfone filters (Pall Life Science) prior to analysis. Concentrations of $Br^-$ and $Cl^-$ were measured by ion chromatography (Dionex Corp.). DOC concentrations were determined by high-temperature combustion and IR measurement of $CO_2$ released (Shimadzu TOC analyzer). Total dissolved N (TDN) was determined using persulphate digestion followed by colorimetric analysis on a flow analyzer (Astoria-Pacific). Ammonia and nitrate were also determined on the flow analyzer with colorimetric analysis. Concentrations of DON were estimated by subtracting $NH_4^+$-N and $NO_3^-$ -N from TDN.

Ultraviolet (UV) absorbance and fluorescence spectra were analyzed to estimate the compositional characteristics of DOM present in the column effluent. Samples at the beginning and the end of the first rainfall (R1-1 and R1-15) and third rainfall (R3-1 and R3-15) were selected for the spectroscopic analysis. Water samples collected during the second rainfall (i.e., R2-1 and R2-15) of the low-temperature treatment (T-5) and room-temperature treatment (T-1′) exhibited spectroscopic properties similar to those samples collected during the third rainfall, so we only report measurements from samples R1-1, R1-15, R3-1 and R3-15.

The UV absorbance spectra were measured using a UV spectrophotometer (Beckman DU 520). The specific UV absorbance ($SUVA_{254}$) was then calculated by dividing the absorbance at 254 nm by the DOC concentration and reported in units of L $mg^{-1}$ $m^{-1}$. $SUVA_{254}$ has been used as a surrogate measurement for DOC aromaticity (*19*).

Fluorescence excitation−emission matrices (EEMs) spectra were obtained using a fluorescence spectrometer (Varian Cary Eclipse). The emission wavelength range was 280−550 nm, while the excitation wavelength was incrementally increased from 220 to 450 nm in 5-nm steps. Before measurement, filtered samples were diluted to a DOC concentration of 4 mg $L^{-1}$ so that the sample absorbance at 254 nm was less than 0.25 $cm^{-1}$. The pH of all diluted samples varied between 4.5 and 5.1. Because the samples had relatively low DOC concentration, and UV−vis absorbance and initial test confirmed that the inner filtering correction had at most an effect of 8%, fluorescence spectra were not further corrected for the inner filtering (*20*). To account for fluctuations in instrumental sensitivity and Raman scattering of water, sample fluorescence intensities were adjusted by subtracting the intensity of the deionized water.

From the EEMs spectra, we also obtained the emission spectra (280−550 nm) at a fixed excitation wavelength of 254 nm. To estimate the extent of humification of effluent DOM, the humification index (HIX) was derived from the emission spectra and defined as the ratio of the emission intensity integration from 435 to 480 nm to the integration from 300 to 345 nm (*21*). High levels of humification may be associated with the presence of condensed aromatic rings, other unsaturated bond systems capable of a high degree of condensation and conjugation, and high molecular weight fractions in the DOM (*22*−*24*).

**2.5. Mathematical Modeling.** We applied a mobile−immobile (MIM) model (*25*) to the time-series data on effluent DOC concentrations to quantify the kinetics of DOC release during the rainfall events. Within our partially saturated soil columns, steady flow and capillary pressures were rapidly established upon elution of only 35 mL of water, which comprises only 10% of the volume of water delivered to the column during the rainfall event (Figures S1−S4 in SI). Given that periods of nonsteady flow associated with soil imbibition (and drainage) were very short, we treated porewater flow as steady in our MIM simulations.

The MIM model is based on the assumption that soil water occurs within inter-aggregate regions, where water is mobile, and intra-aggregate regions, where water is immobile. DOC moves by advection and dispersion in the mobile-water region and exchanges with the immobile-water region by first-order diffusive mass transfer, such that

$$\frac{\partial C_m}{\partial t} + \frac{\rho_b}{\theta_m}\frac{\partial S_m}{\partial t} = D_a\frac{\partial^2 C_m}{\partial X^2} - \frac{q}{\theta^m}\frac{\partial C_m}{\partial X} - \frac{\omega}{\theta_m}(C_m - C_{im}) \quad (1)$$

$$\frac{\partial C_{im}}{\partial t} + \frac{\rho_b}{\theta_{im}}\frac{\partial S_{im}}{\partial t} = \frac{\omega}{\theta_{im}}(C_m - C_{im}) \quad (2)$$

where subscript $m$ and $im$ represent variables in mobile and immobile region, respectively; $C$ is the porewater DOC concentration (mg $L^{-1}$); $t$ is time (h); $\rho_b$ is the soil bulk density (g $L^{-1}$); $\theta$ is the volumetric moisture content ($= \theta_m + \theta_{im}$); $S$ is the readily leachable organic carbon concentration in the solid phase (mg $g^{-1}$), which represents a fraction of the total soil organic matter (*26*); $X$ is the coordinate parallel to flow; $q$ is specific discharge; $\omega$ is the mass transfer rate coefficient for mobile−immobile exchange ($h^{-1}$); and $D_a$ is the hydrodynamic dispersion coefficient.

We assumed that the rates of DOC mobilization and adsorption within the mobile-water and immobile-water regions could be quantified by first-order kinetics equations:

$$\frac{\rho_b}{\theta_m}\frac{\partial S_m}{\partial t} = k_a C_m - \frac{\rho_b}{\theta_m}k_d S_m \quad (3)$$

and

$$\frac{\rho_b}{\theta_{im}}\frac{\partial S_{im}}{\partial t} = k_a C_{im} - \frac{\rho_b}{\theta_{im}}k_d S_{im} \quad (4)$$

where $k_d$ and $k_a$ are first-order rate coefficients ($h^{-1}$) for DOC mobilization and adsorption, respectively.

Equations 1−4 describe the mobilization and transport of DOC within our soil columns. These equations were solved numerically using a Crank−Nicholson finite-difference method for a third-type upper boundary condition and a zero gradient in DOC concentration at the column base. During rainfall interruption intervals, the porewater velocities were modified to simulate zero flow within the columns.

Several parameters must be specified to run the model for DOC transport. Values of $k_d$, $k_a$, and $\omega$ were estimated from the DOC breakthrough data using a Levenberg−Marquadt least-squares algorithm. The parameters $\theta_m$ and $\alpha_L$ were estimated separately from the DOC data by least-squares inversion of the $Cl^-$ breakthrough data. The specific discharge ($q$) was determined from the measured volumetric discharge and $\theta_{im}$ was computed as the difference between the measured, column-averaged moisture content ($\theta$)and the best-fit value of $\theta_m$. Finally, the initial concentrations of the readily leachable organic carbon ($S_{m|}$, $S_{im|}$) were estimated with $k_d$, $k_a$, and $\omega$ in the model inversion of the reference treatments and kept the same for the remaining treatments. Model inversions conducted with different initial guesses for the adjustable parameters converged to the same best-fit parameter values, suggesting that DOC breakthrough data were sufficient to constrain the parameter estimates.

## 3. Results and Discussion

**3.1. Influence of Rainfall Characteristics and Temperature on DOC Mobilization.** Infiltration of artificial rainwater mobilized appreciable quantities of DOC from the A-horizon soil under all conditions tested in this study (Figure 1A and B). The highest DOC concentrations exceeded 90 mg $L^{-1}$ in every experiment and were recorded near the beginning of rainfall events as downward-propagating wetting fronts exited the column. Following passage of the wetting front, effluent DOC concentrations declined rather precipitously as porewater flow stabilized with the continuation of rainfall, but remained above 10 mg $L^{-1}$ for the duration of rainfall and until outflow ceased (Figure 1A and B). Porewater DOC concentrations increased during no-flow periods that separated the rainfall events such that DOC concentrations in effluent samples collected shortly after resumption of rainfall nearly equaled the maximum DOC concentrations observed during the preceding rainfall period (Figure 1A and B). For a given treatment, temporal patterns in DOC concentrations were similar among the three rainfall events with less than a 20% variation in peak DOC concentrations, suggesting that supply of readily leachable DOC was not depleted during the course of our experiments.

Rainfall intensity and frequency affected the quantity of DOC mobilized by infiltrating water. The total mass of DOC eluted from the soil columns increased by 21% as rainfall intensity decreased from 2.9 to 1.0 cm $h^{-1}$ and increased by 25% as the interruption interval increased from 39 to 147 h (Table 2). The differences in DOC concentrations measured in experiments distinguished by rainfall intensity remained approximately constant over an infiltration event (Figure 1A). In contrast, differences in DOC concentration measured in experiments distinguished by rainfall interruption interval decreased from at least 24 mg $L^{-1}$ at the onset of a rainfall event to less than 4 mg $L^{-1}$ at the end of a rainfall event (Figure 1A).

Extended dry periods, in addition to short-term rainfall interruption intervals ranging in duration from several hours

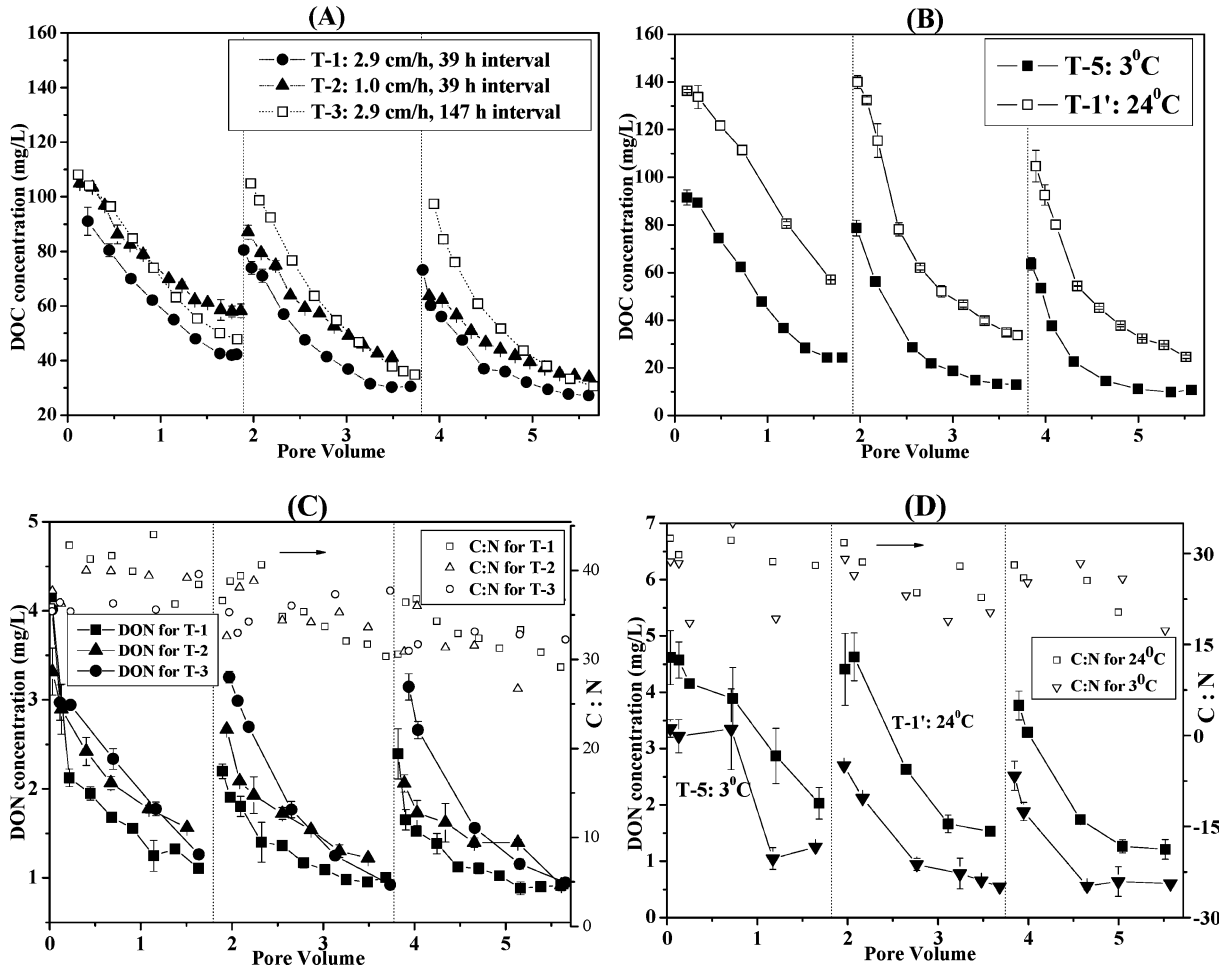


**FIGURE 1. Temporal changes in effluent concentrations of DOC and DON (lines with symbols) and C:N ratios (symbols) over three rainfall events as influenced by rainfall characteristics (A and C) and temperature (B and D). A pore volume equals 175 mL. The vertical dotted lines denote rainfall interruption. Error bars denote standard deviations for duplicate experiments.**

**TABLE 2. Total Eluted Mass of DON and DOC and Average C:N Ratios of DOM for Rainfall Events R1, R2, and R3**

| | | | C:N ratio | | |
|---|---|---|---|---|---|
| treatment | DOC (mg) | DON (mg) | R1 | R2 | R3 |
| T-1 | 51 | 1.38 | 40 | 36 | 34 |
| T-2 | 61.7 | 1.74 | 39 | 35 | 31 |
| T-3 | 63.7 | 1.87 | 35 | 35 | 31 |
| T-1′ | 72.8 | 2.67 | 30 | 26 | 25 |
| T-5 | 35.3 | 1.54 | 23 | 24 | 22 |
| T-7 | 142.4 | 7.30 | 22 | 17 | 18 |
| T-6 | 55.1 | 3.39 | 21 | 14 | 13 |

to several days, affected the DOC mobilization. The second reference experiment in which the soil was stored at 6 °C for 23 weeks prior to rainfall application (T-1′) mimics a wintertime period free of appreciable rainfall or snowmelt. Comparison of treatments T-1 and T-1′ reveal that the extended cold-and-dry period promoted a 43% increase in eluted DOC mass relative to the case in which the soil was stored for only 2 weeks prior to rainfall application. This storage effect may reflect fungal- and bacterial-induced decomposition of soil organic matter (OM). The extracellular enzymes produced by microorganisms catalyze the breakdown of soil OM (*27*), and soil microbial activity can persist at temperatures close to 0 °C (*28*). Although the airtight storage could have promoted the reductive-dissolution of Fe- and Mn-oxyhydroxide surfaces that bind DOC, effluent concentrations of aqueous-phase Fe and Mn in experiment T1′ were low and similar to those measured in experiment T1, suggesting that reductive-dissolution of oxyhydroxides during soil storage contributed little to DOC release.

Changes in temperature promoted considerable changes in DOC mobilization. In particular, a decrease in temperature from 24 to 3 °C reduced maximum DOC concentrations by 45 mg/L (Figure 1B). The total mass of DOC eluted during the three rainfall events was 2-fold higher at 24 °C than at 3 °C owing to sustained differences in effluent concentrations (Table 2).

We attempted to resolve the role of biotic processes in regulating DOC mobilization by comparing results from experiments conducted at 24 and 3 °C with sterile and unsterile soils. DOC concentrations measured in the sterile-soil experiments exceeded 200 mg $L^{-1}$ in some effluent samples (Figure S6 in SI) and were much higher than concentrations observed in the corresponding experiments with the unsterilized soils (Figure 1B). The elevated DOC concentrations in the sterile experiments likely reflect mobilization of organic constituents following radiation-induced cell lysis (*16*), degradation of soil OM (*17*), and reductive-dissolution of organic-matter sorbents (e.g., Fe-oxyhydroxides) (*29*). Although soil sterilization artificially enhanced DOC mobilization, effluent DOC concentrations exhibited the same temporal trends in the experiments with sterile and nonsterile soils, and the temperature effect on DOC mobilization was consistent with more than twice the mass of DOC mobilized at 24 °C than at 3 °C in both the sterile and nonsterile treatments (Table 2). These similarities suggest that, at least for the short time scales evaluated in

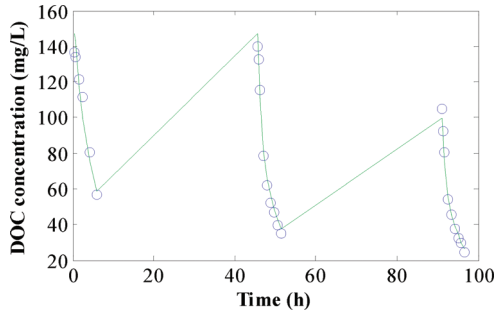


**FIGURE 2. Model simulation of DOC mobilization and transport. The solid line denotes model calculations and the symbols represent effluent DOC measured in treatment T-1′. $R^2$ values that quantify the goodness of model fit to data measured in this experiment and in the other six experiments are presented in Table 1.**

these particular experiments (i.e., tens of hours), abiotic processes are principally responsible for regulating DOC mobilization, and physicochemical responses to temperature decreases, such as reductions in desorption rates, diffusional mass-transfer rates, and DOC solubility, govern the observed temperature effect on rainfall-induced DOC mobilization.

**3.2. Model Simulation and DOM Mobilization Kinetics.** The model-calculated effluent concentrations of DOC and chloride match the corresponding data from the experiments reasonably well ($R^2$ values in Table 1; Figures 2 and S5). The good agreement between measured and modeled DOC concentrations indicates that the two-region model incorporating a first-order rate law for DOC mobilization from soil−water interfaces is capable of describing the mobilization and transport of DOC in aggregated soils. Best-fit estimates of $k_d$, the mobilization rate coefficient, vary between 0.10 and 0.44 $h^{-1}$, which translates to time scales for DOC release ($k_d^{-1}$) ranging from 2 to 10 h. These time scales are similar to the residence time of water in the soil column during a rainfall (= 2−7 h), revealing that DOC leaching was a rate-limited process in our experiments. The rate-limited mobilization accounts for the lower concentrations of DOC eluted from columns that were subjected to the higher rainfall intensity. Few published estimates of DOC mobilization rates are available; however, our best-fit values of $k_d$ are an order of magnitude greater than those reported for DOC mobilization from a sandy soil collected in Germany (*9*). This comparison reveals that a wide range of DOC mobilization rates are likely to be encountered among natural soil systems, which collectively exhibit tremendous variability in hydrological and biogeochemical conditions.

The decrease in temperature (from 24 to 3 °C) causes a 3-fold decrease in $k_d$. To elucidate the rate-limiting mechanism of DOC mobilization during advective-dispersive flow, we used the Arrhenius equation to estimate the apparent desorption activation energy from the temperature dependence of the DOC mobilization rate:

$$k_d(T) = k_0 \exp\left(-\frac{E_{app,d}}{RT}\right) \quad (5)$$

where $k_0$ is the Arrhenius preexponential factor, $E_{app,d}$ is the apparent activation energy of the mobilization process (kJ $mol^{-1}$), $R$ is the universal gas constant, and $T$ is the temperature (K). Accordingly, $E_{app,d}$ can be computed from two individual temperatures ($T_1$ = 297K and $T_2$ = 276K) by

$$E_{app,d} = -R\left(\frac{T_1 T_2}{T_1 - T_2}\right)\ln\left(\frac{k_d(T_2)}{k_d(T_1)}\right) \quad (6)$$

The estimated apparent activation energy, 34 kJ $mol^{-1}$, for DOC mobilization in our experimental system is comparable to the values calculated by Reemtsma (*7*), 26−38 kJ $mol^{-1}$, for soils taken from wastewater infiltration site. This relatively low activation energy suggests that DOC mobilization at the soil−water interfaces is a diffusion-controlled mass transfer process, while high $E_{app,d}$ values usually indicate surface-controlled processes, such as dissolution (*30*). We infer that the DOM mobilization rates, as quantified by $k_d$, are controlled by diffusion across thin films of water that surround soil grains and perhaps by diffusion from intra-aggregate regions that are directly exposed (connected) to mobile-water zones by short diffusional path lengths (*31*). According to the theory of Hayduk and Laudie (*32*), an increase in temperature from 3 to 24 °C would promote an increase in the diffusion coefficients of aqueous-phase organic molecules by a factor of 2.3, which is in close agreement with the observed change in $k_d$ (Table 1).

Best-fit values of $\omega$, the mass transfer rate coefficient for mobile−immobile exchange, increase from $4 \times 10^{-4}$ $h^{-1}$ at 3 °C to $4.4 \times 10^{-3}$ $h^{-1}$ at 24 °C (Table 1). Calculated time scales for this diffusive mass transfer ($\omega^{-1}$) are on the order of 230−2500 h, which are 2 orders of magnitude greater than the residence time of water during a rainfall event (2−7 h). Contributions from this mass transfer can thus be neglected during an individual rainfall event. During the flow-interruption periods, however, slow diffusion from intra-aggregate regions along comparatively long or convoluted pathways may contribute DOC to interaggregate regions that are readily flushed upon resumption of flow. This mobile−immobile exchange, then, replenishes the supply of readily transportable DOC and is responsible for the elevated DOC concentrations observed in the first effluent samples collected after rainfall reinitiation.

Under the same temperature, the best-fit values of $k_d$ and $\omega$ vary with the rainfall intensity and interruption interval. According to Young and Ball (*33*), if a first-order mass transfer model is used to approximate a diffusion-driven process, then the rate coefficient will be a function of not only the intrinsic diffusion rate but also of system parameters including the porewater velocity and the duration of the experiment. Our model results are consistent with their theory and show that both $k_d$ and $\omega$ decrease with lower rainfall intensity and longer interruption interval.

**3.3. Structural Characteristics of DOM.** Fluorescence spectra of all selected samples present two intensity peaks in the EEM plots (Figure S7 in SI). The emission wavelengths of both peaks range from 440 to 470 nm, while the excitation wavelengths of the highest peak and the local peak are located around 230 and 330 nm, respectively. Various DOM fractions have EEMs peaks located at different wavelength pairs, and the EEMs plots in this study closely resemble those of soil standard fulvic acids (*34*). As the ratios between the two peak intensities vary between 1.7 and 1.9 among samples, these two peaks probably reveal the presence of two fluorophores in the fulvic acids (*35*). Although the chemical structures of these fluorophores are not known, quinone moieties may be important and responsible for electron transfer reactions which significantly contribute to the fluorescence of humic substances (*36*).

Across all treatments, EEMs peaks shifted 10−15 nm to longer emission wavelengths between the beginning and the end of a particular rainfall event (Figure S7; Table 3), and the $SUVA_{254}$ and HIX values increased by more than 25% over this time interval. These shifts in spectroscopic properties indicate that molecules with lower aromaticity, less condensed structure, and lower molecular weight are mobilized preferentially (i.e., earlier in elution). Although values of $SUVA_{254}$ and HIX increased over a single rainfall event, they did not increase monotonically over an entire experiment (i.e., across all three rainfall events), but rather decreased between effluent samples separated by a rainfall-interruption

**TABLE 3. Spectroscopic Characteristics of Selected Samples**

| | | | fluorescence characteristics | |
|---|---|---|---|---|
| treatment | sample[a] | SUVA[b] (L $m^{-1}$ $mg^{-1}$) | HIX[b] | EEM peak EX/EM[c] (nm) |
| | R1-1 | 4.0 (0.0) | 30 (2) | 230/445 |
| T-1 | R1-15 | 5.1 (0.1) | 44 (5) | 230/455 |
| | R3-1 | 4.8 (0.1) | 34 (1) | 230/455 |
| | R3-15 | 5.4 (0.2) | 46 (2) | 230/460 |
| T-2 | R1-1 | 4.3 (0.0) | 38 (2) | 230/450 |
| | R1-15 | 5.2 (0.0) | 43 (3) | 230/455 |
| | R3-1 | 4.5 (0.0) | 33 (4) | 230/455 |
| | R3-15 | 5.3 (0.0) | 36 (3) | 230/460 |
| T-3 | R1-1 | 4.5 (0.0) | 31 (1) | 230/445 |
| | R1-15 | 5.7 (0.2) | 48 (1) | 230/455 |
| | R3-1 | 4.7 (0.2) | 37 (3) | 230/455 |
| | R3-15 | 5.7 (0.0) | 46 (4) | 230/465 |
| T-1′ | R1-1 | 4.4 (0.0) | 30 (3) | 230/450 |
| | R1-15 | 5.9 (0.1) | 53 (1) | 230/465 |
| | R3-1 | 5.4 (0.1) | 22 (4) | 230/460 |
| | R3-15 | 6.3 (0.0) | 49 (2) | 230/470 |
| T-5 | R1-1 | 4.6 (0.1) | 20 (2) | 230/450 |
| | R1-15 | 5.8 (0.1) | 51 (2) | 230/465 |
| | R3-1 | 5.4 (0.3) | 16 (1) | 230/460 |
| | R3-15 | 6.1 (0.1) | 44 (2) | 230/470 |

[a] R1: first rainfall; R3: third rainfall. [b] Standard errors are provided in parentheses. [c] EX: excitation wavelength; EM: emission wavelength. Only the highest fluorescence peak of EEM is shown in this table. The local fluorescence peak follows the same temporal pattern as the highest peak in each treatment.

interval (Table 3). Hence, DOM leached immediately after resumption of rainfall was less aromatic and likely to be of lower molecular weight than DOM eluted just prior to the rainfall interruption. Given that smaller components of the DOM pool would move more readily through small, convoluted pore spaces, this behavior is consistent with our hypothesis that DOM flushed from the soil upon resumption of rainfall is supplied to advective-transport pathways during the preceding interruption period by diffusion from the intra-aggregate (immobile-water) zones.

Temperature and an extended cold-and-dry period affected the structure of mobilized DOM, whereas rainfall characteristics did not. HIX values were lower for DOM mobilized at 3 °C than at 24 °C (Table 3), suggesting that DOM mobilized at low temperatures was less condensed and lower in molecular weight. This temperature effect may arise as high-molecular-weight components of the DOM pool with comparatively low diffusivities are rendered effectively immobile when a decrease in temperature further reduces their diffusivities and hence diffusion-limited release into the advecting porewater (*32*). Soils subjected to an extended cold-and-dry period tended to leach DOM with higher $SUVA_{254}$ values (Table 3), suggesting an enrichment of aromatic moieties in the dissolvable OM pool. Previous decomposition studies using litter and soil organic matter reported a similar phenomenon and suggested that these aromatic compounds mainly derive from lignin (*37*).

**3.4. Comparison of DON and DOC Mobilization.** The characteristics of DON mobilization were qualitatively similar to the characteristics of DOC mobilization (Figure 1C and D). Effluent DON concentrations for unsterilized soils peaked at 3−5 mg $L^{-1}$ shortly after rainfall initiation and then rapidly declined to 1−2 mg $L^{-1}$. The total mass of DON eluted from the columns of unsterilized soil ranged from 1.38 to 2.67 mg and was 23−37-fold less than the mass of DOC eluted (Table 2). Similarly to DOC mobilization, more DON was mobilized at higher temperature, under lower rainfall intensity, and at longer rainfall interruption intervals.

The C:N ratios of effluent DOM, which ranged from 15 to 45 (Table 2), indicate the relative quantities of DOC and DON that were transported through the soil. During successive rainfall events, the DOC:DON ratios were approximately constant in the treatment T-3 and exhibited a slight downward trend with cumulative rainfall volume in the remaining four treatments (symbols in Figure 1C and D). The increase in content of DON relative to DOC with time suggests that nitrogenous components are less susceptible to mobilization and thus are transported more slowly through the soil profile during infiltration events. This behavior may reflect that some N-containing functional groups have a strong affinity for sediment surfaces (*38*). Alternatively, Kaiser (*39*) suggested that the sorption of DON may be favored by acidic groups, such as carboxylic acid groups and perhaps phenolic groups, rather than by N-containing amino groups.

Among unsterilized soil treatments, changes in storage time had the most notable influence on the C:N ratios of effluent DOM. The average DOC:DON ratio decreased by 36% when storage time increased from 2 to 23 weeks (Table 2), suggesting that dissolvable organic C and N were produced in unfixed ratios and the production rate of dissolvable organic N is greater than that of dissolvable organic C in the absence of leaf litter and root input.

In conclusion, our findings demonstrate that quantities of DOM mobilized in response to rainfall increase with temperature and decrease with rainfall intensity and frequency. We also find that the structure of mobilized DOM, as characterized by ultraviolet (UV) absorbance and fluorescence spectra and C:N ratio, is sensitive to these factors, and that DOM becomes more condensed and aromatic and lower in C:N through the course of a precipitation event. Comparison of DOM measurements made in the experiments to model calculations suggests that diffusional mechanisms regulate the rate of DOC mobilization during precipitation events and replenish the depleted mobile-water DOM pool between infiltration events through the slow delivery of DOM from intra-aggregate to inter-aggregate soil water regions. The observed sensitivity of these diffusional mechanisms to temperature suggests that seasonal variations in DOC export from temperate-zone watersheds may reflect temperature regulation of physicochemical processes, in addition to the better-known effects of biotic processes, such as leaf-litter input and organic-matter decomposition.

## Acknowledgments

We thank Yang Qiu, Ying Zhang, Xuemei Han, and Emery Boose for help in soil sampling and Jonas Karosas for help with DON analyses. We are especially grateful for the constructive comments provided by three anonymous reviewers. This research was supported through Department of Energy Grants DE-FG02-08ER64638 and ER64804.

## Supporting Information Available

Measurements and computations of porewater flow (Figure S1), capillary pressure (Figure S2), soil-water retention characteristics (Figure S3), volumetric moisture content (Figure S4), chloride breakthrough (Figure S5), effluent DOC and DON concentrations in the sterile-soil experiments (Figure S6), fluorescence EEM spectra (Figure S7), and model parameters (Table S1). This material is available free of charge via the Internet at http://pubs.acs.org.

## Literature Cited

(1) Kalbitz, K.; Solinger, S.; Park, J. H.; Michalzik, B.; Matzner, E. Controls on the dynamics of dissolved organic matter in soils: A review. *Soil Sci.* **2000**, *165* (4), 277–304.

(2) McDowell, W. H.; Likens, G. E. Origin, Composition, and Flux of Dissolved Organic-Carbon in the Hubbard Brook Valley. *Ecol. Monogr.* **1988**, *58* (3), 177–195.

(3) Hinton, M. J.; Schiff, S. L.; English, M. C. The significance of storms for the concentration and export of dissolved organic carbon from two Precambrian Shield catchments. *Biogeochemistry* **1997**, *36* (1), 67–88.
(4) Inamdar, S. P.; O'Leary, N.; Mitchell, M. J.; Riley, J. T. The impact of storm events on solute exports from a glaciated forested watershed in western New York, U.S.A. *Hydrol. Process* **2006**, *20* (16), 3423–3439.
(5) Dawson, J. J. C.; Soulsby, C.; Tetzlaff, D.; Hrachowitz, M.; Dunn, S. M.; Malcolm, I. A. Influence of hydrology and seasonality on DOC exports from three contrasting upland catchments. *Biogeochemistry* **2008**, *90* (1), 93–113.
(6) Lumsdon, D. G.; Stutter, M. I.; Cooper, R. J.; Manson, J. R. Model assessment of biogeochemical controls on dissolved organic carbon partitioning in an acid organic soil. *Environ. Sci. Technol.* **2005**, *39* (20), 8057–8063.
(7) Reemtsma, T.; Bredow, A.; Gehring, M. The nature and kinetics of organic matter release from soil by salt solutions. *Eur. J. Soil Sci.* **1999**, *50* (1), 53–64.
(8) Stutter, M. I.; Lumsdon, D. G.; Thoss, V. Physico-chemical and biological controls on dissolved organic matter in peat aggregate columns. *Eur. J. Soil Sci.* **2007**, *58* (3), 646–657.
(9) Wehrer, M.; Totsche, K. U. Determination of effective release rates of polycyclic aromatic hydrocarbons and dissolved organic carbon by column outflow experiments. *Eur. J. Soil Sci.* **2005**, *56* (6), 803–813.
(10) Andersson, S.; Nilsson, S. I.; Saetre, P. Leaching of dissolved organic carbon (DOC) and dissolved organic nitrogen (DON) in mor humus as affected by temperature and pH. *Soil Biol. Biochem.* **2000**, *32* (1), 1–10.
(11) Christ, M. J.; David, M. B. Temperature and moisture effects on the production of dissolved organic carbon in a Spodosol. *Soil Biol. Biochem.* **1996**, *28* (9), 1191–1199.
(12) Godde, M.; David, M. B.; Christ, M. J.; Kaupenjohann, M.; Vance, G. F. Carbon mobilization from the forest floor under red spruce in the northeastern U.S.A. *Soil Biol. Biochem.* **1996**, *28* (9), 1181–1189.
(13) Bartschat, B. M.; Cabaniss, S. E.; Morel, F. M. M. Oligoelectrolyte model for cation binding by humic substances. *Environ. Sci. Technol.* **1992**, *26* (2), 284–294.
(14) Marschner, B.; Kalbitz, K. Controls of bioavailability and biodegradability of dissolved organic matter in soils. *Geoderma* **2003**, *113* (3−4), 211–235.
(15) Michalzik, B.; Matzner, E. Dynamics of dissolved organic nitrogen and carbon in a Central European Norway spruce ecosystem. *Eur. J. Soil Sci.* **1999**, *50* (4), 579–590.
(16) Berns, A. E.; Philipp, H.; Narres, H. D.; Burauel, P.; Vereecken, H.; Tappe, W. Effect of gamma-sterilization and autoclaving on soil organic matter structure as studied by solid state NMR, UV and fluorescence spectroscopy. *Eur. J. Soil Sci.* **2008**, *59* (3), 540–550.
(17) McNamara, N. P.; Black, H. I. J.; Beresford, N. A.; Parekh, N. R. Effects of acute gamma irradiation on chemical, physical and biological properties of soils. *Appl. Soil Ecol.* **2003**, *24* (2), 117–132.
(18) Guo, M. X.; Chorover, J. Transport and fractionation of dissolved organic matter in soil columns. *Soil Sci.* **2003**, *168* (2), 108–118.
(19) Weishaar, J. L.; Aiken, G. R.; Bergamaschi, B. A.; Fram, M. S.; Fujii, R.; Mopper, K. Evaluation of specific ultraviolet absorbance as an indicator of the chemical composition and reactivity of dissolved organic carbon. *Environ. Sci. Technol.* **2003**, *37* (20), 4702–4708.
(20) Zsolnay, A. Dissolved organic matter: artefacts, definitions, and functions. *Geoderma* **2003**, *113* (3−4), 187–209.
(21) Ohno, T. Fluorescence inner-filtering correction for determining the humification index of dissolved organic matter. *Environ. Sci. Technol.* **2002**, *36* (4), 742–746.
(22) Kalbitz, K.; Geyer, W.; Geyer, S. Spectroscopic properties of dissolved humic substances - a reflection of land use history in a fen area. *Biogeochemistry* **1999**, *47* (2), 219–238.
(23) Senesi, N.; Miano, T. M.; Provenzano, M. R.; Brunetti, G. Characterization, Differentiation, and Classification of Humic Substances by Fluorescence Spectroscopy. *Soil Sci.* **1991**, *152* (4), 259–271.
(24) Hur, J.; Lee, D. H.; Shin, H. S. Comparison of the structural, spectroscopic and phenanthrene binding characteristics of humic acids from soils and lake sediments. *Org. Geochem.* **2009**, *40* (10), 1091–1099.
(25) Vangenuchten, M. T.; Wierenga, P. J. Mass-Transfer Studies in Sorbing Porous-Media 0.1. Analytical Solutions. *Soil Sci. Soc. Am. J.* **1976**, *40* (4), 473–480.
(26) Corvasce, M.; Zsolnay, A.; D'Orazio, V.; Lopez, R.; Miano, T. M. Characterization of water extractable organic matter in a deep soil profile. *Chemosphere* **2006**, *62* (10), 1583–1590.
(27) Schimel, J. P.; Weintraub, M. N. The implications of exoenzyme activity on microbial carbon and nitrogen limitation in soil: a theoretical model. *Soil Biol. Biochem.* **2003**, *35* (4), 549–563.
(28) Sommerfeld, R. A.; Mosier, A. R.; Musselman, R. C. $CO_2$, $CH_4$ and $N_2O$ Flux through a Wyoming Snowpack and Implications for Global Budgets. *Nature* **1993**, *361* (6408), 140–142.
(29) Bank, T. L.; Kukkadapu, R. K.; Madden, A. S.; Ginder-Vogel, M. A.; Baldwin, M. E.; Jardine, P. M. Effects of gamma-sterilization on the physico-chemical properties of natural sediments. *Chem. Geol.* **2008**, *251* (1−4), 1–7.
(30) Sparks, D. L. *Environmental Soil Chemistry*, 2nd ed.; Academic Press: San Diego, CA, 2003.
(31) Werth, C. J.; Reinhard, M. Effects of temperature on trichloroethylene desorption from silica gel and natural sediments 0.2. Kinetics. *Environ. Sci. Technol.* **1997**, *31* (3), 697–703.
(32) Hayduk, W.; Laudie, H. Prediction of diffusion-coefficients for nonelectrolytes in dilute aqueous-solutions. *AICHE J.* **1974**, *20* (3), 611–615.
(33) Young, D. F.; Ball, W. P. Effects of column conditions on the first-order rate modeling of nonequilibrium solute breakthrough. *Water Resour. Res.* **1995**, *31* (9), 2181–2192.
(34) Alberts, J. J.; Takacs, M. Total luminescence spectra of IHSS standard and reference fulvic acids, humic acids and natural organic matter: comparison of aquatic and terrestrial source terms. *Org. Geochem.* **2004**, *35* (3), 243–256.
(35) Coble, P. G.; Green, S. A.; Blough, N. V.; Gagosian, R. B. Characterization of dissolved organic-matter in the Black-Sea by fluorescence spectroscopy. *Nature* **1990**, *348* (6300), 432–435.
(36) Cory, R. M.; McKnight, D. M. Fluorescence spectroscopy reveals ubiquitous presence of oxidized and reduced quinones in dissolved organic matter. *Environ. Sci. Technol.* **2005**, *39* (21), 8142–8149.
(37) Kogel-Knabner, I. The macromolecular organic composition of plant and microbial residues as inputs to soil organic matter. *Soil Biol. Biochem.* **2002**, *34* (2), 139–162.
(38) Mcknight, D. M.; Bencala, K. E.; Zellweger, G. W.; Aiken, G. R.; Feder, G. L.; Thorn, K. A. Sorption of Dissolved Organic-Carbon by Hydrous Aluminum and Iron-Oxides Occurring at the Confluence of Deer Creek with the Snake River, Summit County, Colorado. *Environ. Sci. Technol.* **1992**, *26* (7), 1388–1396.
(39) Kaiser, K.; Zech, W. Sorption of dissolved organic nitrogen by acid subsoil horizons and individual mineral phases. *Eur. J. Soil Sci.* **2000**, *51* (3), 403–411.

ES1002296